

# Pressure-induced tuning of a magnetic phase separation in $\text{Nd}_{0.53}\text{Sr}_{0.47}\text{MnO}_3$

M. Baldini,<sup>1</sup> Y. Ding,<sup>2</sup> S. Wang,<sup>3</sup> Y. Lin,<sup>3</sup> C. A. Tulk,<sup>4</sup> A. M. dos Santos,<sup>5</sup> J. F. Mitchell,<sup>6</sup> D. Haskel,<sup>2</sup> and W. L. Mao<sup>3,7,8</sup>

<sup>1</sup>*HPSynC, Geophysical Laboratory, Carnegie Institution of Washington, 9700 S. Cass Avenue, Argonne, Illinois 60439, USA*

<sup>2</sup>*Advanced Photon Source, Argonne National Laboratory, Argonne, Illinois 60439, USA*

<sup>3</sup>*Geological and Environmental Sciences, Stanford University, California 94025, USA*

<sup>4</sup>*Chemical and Engineering Materials Division, Neutron Sciences Directorate, Oak Ridge National Laboratory, Oak Ridge, Tennessee 37831*

<sup>5</sup>*Quantum Condensed Matter Division Neutron Sciences Directorate, Oak Ridge National Laboratory, Oak Ridge, Tennessee 37831*

<sup>6</sup>*Materials Science Division, Argonne National Laboratory, Argonne, Illinois 60439, USA*

<sup>7</sup>*Stanford Institute for Materials and Energy Science, SLAC National Accelerator Laboratory, 2575 Sand Hill Road, Menlo Park, 94025 California, USA*

<sup>8</sup>*Photon Science, SLAC National Accelerator Laboratory, Menlo Park, California 94025, USA*

(Received 17 April 2012; revised manuscript received 21 August 2012; published 6 September 2012)

X-ray magnetic circular dichroism and neutron diffraction measurements were conducted *in situ* at high pressure and low temperature to investigate the evolution of the magnetic properties of  $\text{Nd}_{0.53}\text{Sr}_{0.47}\text{MnO}_3$  (NSMO47). The neutron diffraction data provide the experimental evidence for the presence of antiferromagnetic domains within the conducting ferromagnetic host at ambient pressure. The antiferromagnetic phase becomes dominant above 3 GPa with a concomitant reduction of the FM phase. Those findings indicate that the magnetic ground state of NSMO47 is more complex than previously reported, confirming the coexistence of competing phases over the doping range in which colossal magnetoresistance is observed. We also find that magnetic phase separation in the form of domains appears to be an intrinsic phenomenon at high pressure.

DOI: [10.1103/PhysRevB.86.094407](https://doi.org/10.1103/PhysRevB.86.094407)

PACS number(s): 62.50.-p, 75.47.Lx, 64.75.Jk, 75.75.-c

## I. INTRODUCTION

Since the discovery of colossal magnetoresistance (CMR), rare-earth manganites have been the subject of significant experimental and theoretical efforts. The strong coupling between lattice, orbital, electronic, and spin degrees of freedom makes manganites ideal compounds for studying the complex phenomena observed in metal oxides.<sup>1</sup> In recent years, theoretical and experimental results have been converging on a unified picture for the physics of manganites in the CMR regimes, which is dominated by the competition between coexisting ferromagnetic (FM) metallic and antiferromagnetic/charge-ordered (AFM/CO) insulating states.<sup>2-5</sup> Direct imaging of nanoscale CO domains in  $\text{La}_{0.55}\text{Ca}_{0.45}\text{MnO}_3$  demonstrate that the volume fraction of these domains is large enough to contribute significantly to the CMR effect.<sup>4</sup> Taking into account the competition between double-exchange ferromagnetic and the charge-ordered insulating phase, a theoretical study found that disorder enhances the insulating nature of these systems at high temperature and thus the CMR effect.<sup>5</sup>

It is therefore crucial to clarify the role played by the super-exchange (SE) interactions, which are responsible for the stabilization of the AFM/CO phase, in connection with other degrees of freedom. High-pressure techniques have been proven to be effective in decoupling interactions in manganites.<sup>6</sup> In particular, pressure increases the strength of the SE interactions favoring the onset and the stabilization of AFM long-range order. In  $\text{La}_{0.75}\text{Ca}_{0.25}\text{MnO}_3$ , suppression of the FM phase was observed at 23 GPa<sup>7</sup> together with the onset of an AFM phase above 2 GPa and subsequent formation of magnetic domains.<sup>8-10</sup>

The  $\text{Nd}_{1-x}\text{Sr}_x\text{MnO}_3$  family is an ideal candidate for high pressure studies since it displays a quite complex magnetic phase diagram with CMR effect for  $0.3 < x < 0.5$ , a stable CO phase for  $x = 0.5$  and an unusual A-type AFM metallic

ground state for  $x > 0.51$ .<sup>11-13</sup> In this work, we focus our attention on the doping range in which CMR is observed studying  $\text{Nd}_{0.53}\text{Sr}_{0.47}\text{MnO}_3$  (NSMO47), which displays a FM metallic ground state ( $T_C \sim 270$  K) and an orthorhombic structure (space group *Ibmm*) at ambient pressure.<sup>11</sup> The pressure evolution of the magnetic properties of NSMO47 was investigated using x-ray magnetic circular dichroism (XMCD) and neutron diffraction techniques. The presence of AFM and FM magnetic domains was observed at ambient pressure by neutron diffraction. XMCD data indicate a strong reduction of the FM phase applying pressure. The volume fraction of the AFM phase was found to increase and become dominant above 3 GPa. The coexistence of competing magnetic ground states even at ambient pressure, provides support for recent theoretical models on the origin of CMR in doped manganites.

## II. EXPERIMENTAL

NSMO47 sample was prepared by standard solid state synthesis starting from  $\text{Nd}_2\text{O}_3$ ,  $\text{SrCO}_3$  and  $\text{MnO}_2$ . The XMCD measurements were performed at beam line 4-ID-D of the Advanced Photon Source (APS), Argonne National Laboratory (ANL) in helicity switching mode (14.3 Hz).<sup>14</sup> The sample was loaded into a membrane-driven diamond cell with perforated anvils and silicone oil used as the pressure-transmitting medium. Pressure was calibrated *in situ* using the fluorescence shift of ruby.<sup>15</sup> The energy of the incident x-ray beam was scanned through the Nd  $L_3$  absorption edge (6208 eV) and data were collected between 1 bar and 8.6 GPa at selected temperatures within the 14–200 K range in a  $H = 0.6$  T applied field. The neutron diffraction data were collected at the SNAP instrument of the Spallation Neutron Source (SNS), Oak Ridge National Laboratory (ORNL). The sample was loaded into a Paris-Edinburgh cell together with

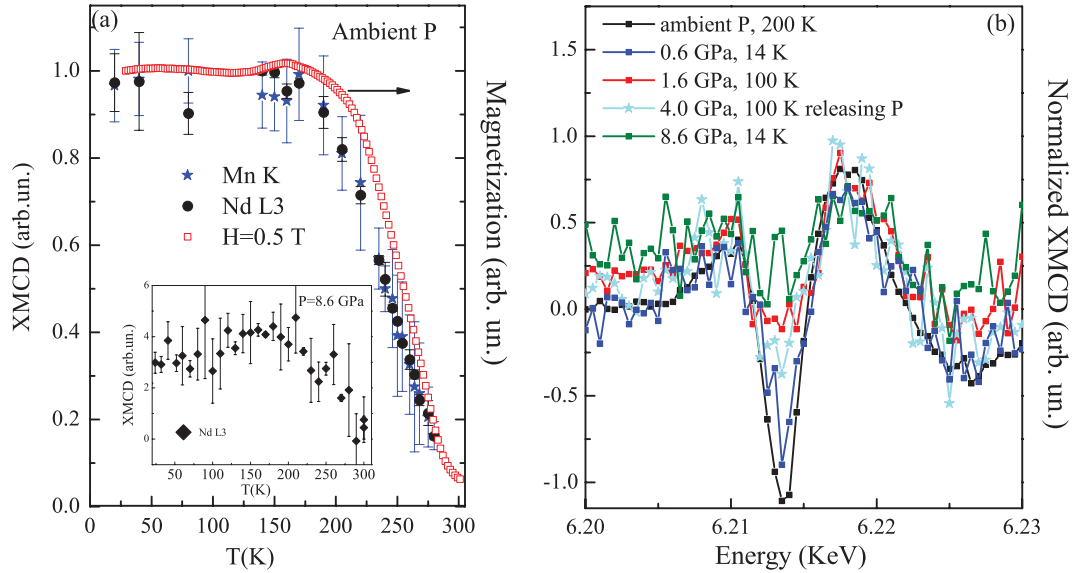


FIG. 1. (Color online) (a) Temperature dependence of Mn *K* (blue stars) and Nd *L*<sub>3</sub> XMCD (black circles) signals collected at ambient pressure. Results obtained performing SQUID magnetization measurements (red squares) are superimposed to the XMCD data. (Inset) Temperature dependence of the Nd *L*<sub>3</sub> XMCD signal at 8.6 GPa, obtained performing XMCD measurements decreasing temperature. (b) Normalized XMCD data at low temperature and different pressures. The data at 4 GPa were collected on decreasing pressure.

NaCl as the pressure-transmitting medium. The equation of state of NaCl was used to determine pressure.<sup>16</sup> The data were collected up to 6.7 GPa at 80 K using two different detectors, one centered at 48.9° and the other at 90°. Two wavelength ranges were used for the time of flight diffraction measurements: (1)  $0.5 \leq \lambda \leq 3.7 \text{ \AA}$  and (2)  $4.5 \leq \lambda \leq 8.3 \text{ \AA}$ , to access a larger *d*-spacing range. The neutron data were then refined using FULLPROF software<sup>17</sup> and lattice parameters and effective magnetic moments were obtained.

### III. EXPERIMENTAL RESULTS AND DISCUSSION

Superconducting quantum interference device (SQUID) magnetization measurements were performed in a  $H = 0.5 \text{ T}$  magnetic field to characterize the sample and determine the Curie temperature  $T_C$  at ambient pressure [see Fig. 1(a)].  $T_C$  was found to be approximately 270 K in good agreement with previous work.<sup>11</sup> Since the Nd *L*<sub>3</sub> edge XMCD signal is stronger than the Mn *K*-edge XMCD signal, we selected the former for pressure-dependent measurements. The strong hybridization between Nd *5d* and Mn *3d* orbitals induces a net spin polarization in the Nd *5d* band. This induced Nd magnetization is proportional to the ordered Mn moment as it is well displayed in Fig. 1(a) where the temperature dependencies of the Mn *K* and Nd *L*<sub>3</sub> XMCD signals collected at ambient pressure are reported together with the SQUID magnetization data. Since no ordering of the Nd *4f* moments is observed, the Nd XMCD signal is only due to the magnetization of Mn atoms and the use of the Nd *L*<sub>3</sub> edge is fully justified. Figure 1(b) shows the normalized XMCD data at different pressures collected well below  $T_C$  at 14 K and 100 K. The data at 4 GPa were collected on decreasing pressure. The strength of XMCD monotonically decreases with pressure. This indicates that either the local moment is reduced in a spatially homogeneous FM phase,

or that the volume fraction of the FM phase is reduced in the presence of magnetic phase separation up to 8.6 GPa. In the inset of Fig. 1(a) the temperature evolution of the the Nd *L*<sub>3</sub> XMCD signal at 8.6 GPa is also reported.  $T_C$  is found not to change at 8.6 GPa ruling out the possibility that the suppression of the XMCD signal is associated with the reduction of Mn local moment and indicating that the volume fraction of the FM phase is reduced with pressure.

The neutron diffraction data further support the phase separation scenario. Low *d*-spacing diffraction patterns (from 0.5 to 4.0 Å) were collected at 88 K between 1 bar and 6.7 GPa (see Fig. 2). Comparing the neutron pattern collected at 300 K and 88 K (see Fig. 2, right inset), a pure magnetic peak is observed at 3.43 Å, whose position is consistent with the presence of an A-type AFM order.<sup>11</sup> The neutron diffraction patterns collected at high *d*-spacings using an incident wavelength range  $4.5 \leq \lambda \leq 8.3 \text{ \AA}$  are displayed in the inset of Fig. 3. Another pure magnetic reflection is observed at around  $d = 7.50 \text{ \AA}$ , whose position confirms the presence of an A-type AFM phase.<sup>11</sup> This is the direct evidence for the presence of an AFM order at ambient pressure in NSMO47. In Ref. 11, the Nd<sub>1-x</sub>Sr<sub>x</sub>MnO<sub>3</sub> phase diagram is reported as a function of doping content but no information is given about the method used to determine  $T_C$  and the ferromagnetic ground state for  $x = 0.47$ . However, the occurrence of dynamic phase segregation within the FM phase has been proposed for NSMO47 based on Mn *2p* resonance photoemission results.<sup>18</sup> A phase separation model in which AFM droplets lie in a conducting FM host was also proposed for Nd<sub>0.55</sub>Sr<sub>0.45</sub>MnO<sub>3</sub>,<sup>19,20</sup> a sample with Sr content and macroscopic properties that are similar to NSMO47. In this regard, it is worth to note that neutron diffraction is a more effective and sensitive technique to directly determine spin arrangements.

The position of the two pure magnetic peaks establishes beyond a doubt that the AFM phase is A-type. This result

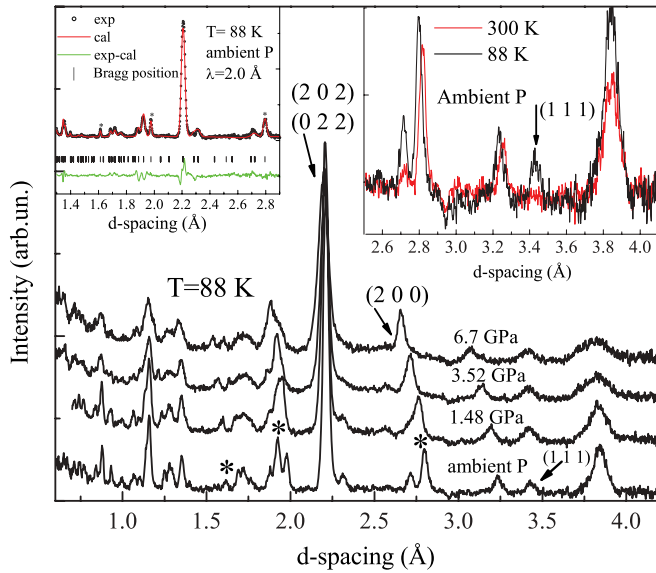


FIG. 2. (Color online) Low  $d$ -spacing neutron diffraction patterns collected at 88 K as a function of pressure. The asterisks indicate peaks from NaCl. The  $(2\ 0\ 2)/(0\ 2\ 2)$  NSMO47, the  $(2\ 0\ 0)$  NaCl, and the  $(1\ 1\ 1)$  pure magnetic peaks are indicated. (Left inset) Rietveld refinement of the neutron pattern collected at ambient pressure and low temperature. (Right inset) Neutron diffraction patterns collected at 300 and 88 K at ambient pressure; the black arrow indicates the pure magnetic peak  $(1\ 1\ 1)$  centered at  $3.43\ \text{\AA}$ .

also makes the possibility of chemical inhomogeneity being responsible for the phase separation very unlikely since a CE-type phase is expected for  $0.49 < x < 0.51$ . The neutron data were then refined using an  $Ibmm$  space group with an associated FM and A-type AFM order and an  $Fm\bar{3}m$  structure for the NaCl contribution to the neutron patterns. The magnetic unit cell was described by four Mn atoms:  $\text{Mn1} = (0, 0, 1/2)$ ,  $\text{Mn2} = (0, 1/2, 1/2)$ ,  $\text{Mn3} = (1/2, 1/2, 0)$ , and  $\text{Mn4} = (1/2, 0, 0)$ . The neutron pattern was calculated using a  $Ry = (+ + - -)$  sequence of magnetic moments and propagation vector  $k = (0, 0, 0)$  for the AFM phase, meaning that the magnetic moments were found to be ordered ferromagnetically on the  $ab$  plane with FM planes antiferromagnetically stacked along the  $c$  axis. The Rietveld refinements are in good agreement with the experimental data (left insets of Figs. 2 and 3). Lattice parameters and values of the FM and AFM effective magnetic moments were obtained.

A further confirmation of intrinsic nature of magnetic phase separation rather than being a result of chemical inhomogeneity is given by the obtained structural information. The lattice parameters [ $a = 5.44(4)\ \text{\AA}$ ,  $b = 5.43(4)\ \text{\AA}$ , and  $c = 7.55(4)\ \text{\AA}$ ] obtained at ambient pressure were found to be in good agreement with those reported in Ref. 21. Indeed, the A-type AFM phase observed in Sr doped  $\text{NdMnO}_3$  manganites for  $x > 0.51$  is accompanied by the onset of a tetragonal crystal structure. No evidence for the presence of a different structure is seen in the neutron diffraction patterns. Only two AFM peaks are observed over the investigated  $d$ -spacing range at ambient pressure, further confirming the phase separation scenario with AFM domains in a conducting ferromagnetic environment. The small bump observed in the

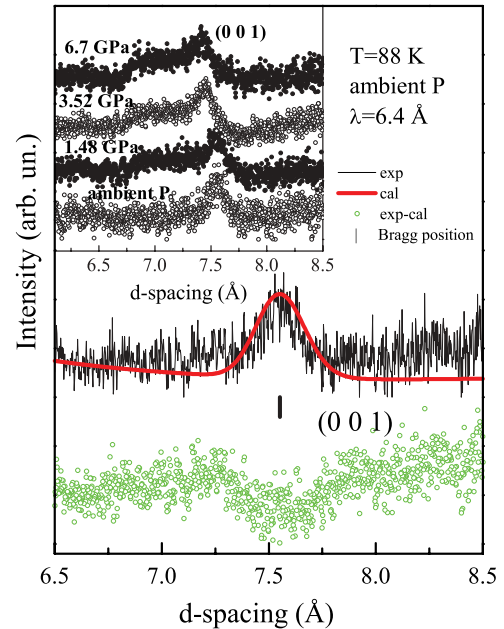


FIG. 3. (Color online) Rietveld refinement of the high  $d$ -spacing neutron pattern collected at ambient pressure and 88 K. (Inset) High  $d$ -spacing neutron diffraction patterns collected at 88 K at different pressures. The broad shoulder observed around  $d = 7\ \text{\AA}$  is a background distortion.

temperature evolution of SQUID magnetization data below 160–170 K [see Fig. 1(a)] is consistent with the presence of an AFM phase below this temperature at ambient pressure. This has broad implications since it reveals that the magnetic ground state for NSMO47 is more complex than previously reported and provides experimental evidence to support the most recent theoretical models on manganites which claim that the presence of competing states is crucial for the occurrence of CMR in hole doped manganites.<sup>1,22</sup> In Fig. 4, the pressure evolution of normalized XMCD integrated intensities, lattice parameters, orthorhombic distortions and FM and AFM effective magnetic moments are reported. The XMCD signal, normalized to the absorption jump, rapidly decreases between 1 bar and 3 GPa and it appears significantly suppressed above 3 GPa [see Fig. 4(a)]. Pressure is more effective in modifying the lattice parameters below 3 GPa where the  $a$  axis elongates and the  $c$  axis is compressed. This uniaxial compression of the  $c$  axis is in good agreement with a well established physical picture. Indeed, the contraction of the  $c$  parameter is consistent with the stabilization of an A-type AFM phase and  $d_{x^2-y^2}$  orbital ordering at high pressure.<sup>7,8,20,23</sup> In this framework, a simple way to quantitatively determine if further distortions are induced by pressure is to calculate the orthorhombic strain. The  $ab$ -plane  $O_{ab}$  and the  $c$ -axis  $O_c$  distortions are defined by  $O_{ab} = 2(a - b)/(a + b)$  and  $O_c = 2(a + b - 2c\sqrt{2})/(a + b + 2c\sqrt{2})$ , respectively.<sup>24</sup> In Fig. 4(c), both distortions are found to increase confirming the uniaxial compression of the  $\text{MnO}_6$  with pressure. The effective magnetic moments obtained by Rietveld refinements are displayed in Fig. 4(d). The FM moment is found to decrease with pressure whereas the opposite trend is observed for the AFM moment. The reduction of the FM moment is

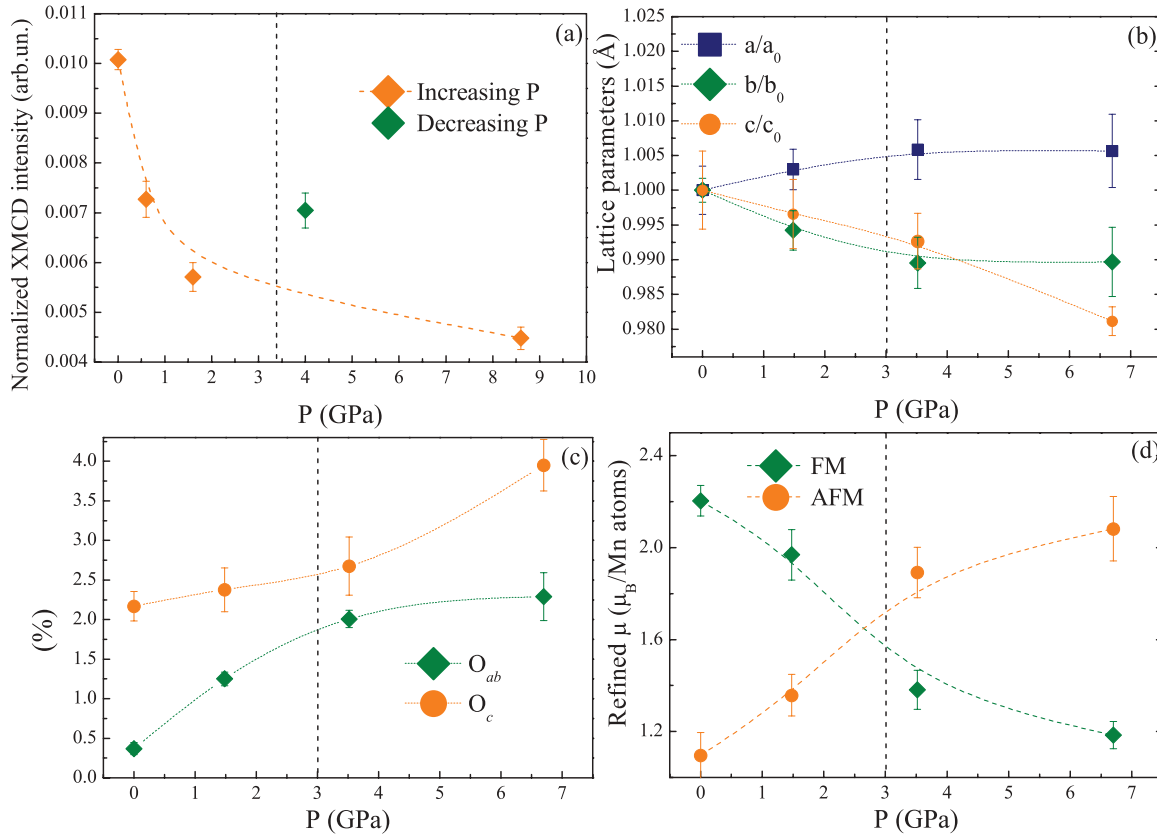


FIG. 4. (Color online) (a) Pressure evolution of the normalized XMCD integrated intensities. The pressure point at 4 GPa was collected decreasing pressure. Pressure dependence of (b) lattice parameters and (c) orthorhombic distortion. (d) Evolution of the FM and AFM effective magnetic moments with pressure. Dashed curves are guides for the eye.

consistent with the pressure evolution of the XMCD magnetic intensities reported in Fig. 4(a). Considering both the XMCD and neutron results, this pressure behavior can be explained only considering that the volume fraction of the A-type AFM phase increases with pressure to the detriment of the FM phase.

In summary, neutron data collected at ambient pressure reveal the presence of A-type AFM domains in a ferromagnetic host, indicating a more complex scenario for NSMO47 and confirming that the presence of competing states is crucial to induce CMR effects. Two different pressure regimes can be identified. There is a lower pressure region below 3 GPa in which the volume fraction of the FM phase is strongly reduced but still dominant over the AFM phase. The changes in XMCD signal and lattice parameters observed above 3 GPa indicate that the A-type AFM phase is dominant over the FM one. The stabilization of the AFM phase is further confirmed by the pressure dependence of the AFM and FM effective magnetic moments. Our results together with recent studies<sup>7,8</sup> indicate that pressure is effective in enhancing SE interactions and emphasize the interplay between structural, magnetic and

orbital degrees of freedom. Our results also provide further evidences that formation of domains at high pressure is an intrinsic phenomenon in manganites.<sup>25</sup>

#### ACKNOWLEDGMENTS

This work was supported as part of the EFree, an Energy Frontier Research Center funded by the US Department of Energy, Office of Science, Office of Basic Energy Sciences under Award No. DE-SG0001057. A portion of this research conducted at SNS ORNL was sponsored by the Scientific User Facilities Division, Office of Basic Energy Sciences, US Department of Energy. Specimen growth and magnetic characterization in the Materials Science Division at ANL supported by U.S. DOE Office of Science Laboratory, Basic Energy Sciences, Materials Science and Engineering Division, under contract No. DE-AC02-06CH211357. We also would like to thank N. Souza-Neto who helped with the XMCD measurements, J. Molaison and N. Pradhan who helped with the neutron diffraction measurements, and H. Zheng who helped with the magnetization measurements.

<sup>1</sup>C. Sen, G. Alvarez, and E. Dagotto, *Phys. Rev. Lett.* **98**, 127202 (2007).

<sup>2</sup>H. Kuwahara, Y. Moritomo, Y. Tomioka, A. Asamitsu, M. Kasai, R. Kumai, and Y. Tokura, *Phys. Rev. B* **56**, 9386 (1997).

<sup>3</sup>E. Dagotto *et al.*, *Phys. Rep.* **344**, 1 (2001); E. Dagotto, *New J. Phys.* **7**, 67 (2005).

<sup>4</sup>J. Tao, D. Niebieskikwiat, M. Varela, W. Luo, M. A. Schofield, Y. Zhu, M. B. Salamon, J. M. Zuo, S. T. Pantelides, and S. J. Pennycook, *Phys. Rev. Lett.* **103**, 097202 (2009).

- <sup>5</sup>Y. Motome, N. Furukawa, and N. Nagaosa, *Lect. Notes Phys.* **678**, 71 (2005).
- <sup>6</sup>P. Postorino, A. Congeduti, P. Dore, A. Sacchetti, F. Gorelli, L. Ulivi, A. Kumar, and D. D. Sarma, *Phys. Rev. Lett.* **91**, 175501 (2003).
- <sup>7</sup>Y. Ding, D. Haskel, Y. C. Tseng, E. Kaneshita, M. van Veenendaal, J. F. Mitchell, S. V. Sinogeikin, V. Prakapenka, and H-K. Mao, *Phys. Rev. Lett.* **102**, 237201 (2009).
- <sup>8</sup>M. Baldini, L. Capogna, M. Capone, E. Arcangeletti, C. Petrillo, I. Goncharenko, and P. Postorino, *J. Phys.: Condens. Matter* **24**, 045601 (2012).
- <sup>9</sup>A. Sacchetti, P. Postorino, and M. Capone, *New J. Phys.* **8**, 3 (2006).
- <sup>10</sup>D. P. Kozlenko, S. E. Kichanova, V. I. Voronin, B. N. Savenko, V. P. Glazkov, E. A. Kiseleva, and N. V. Proskurnina, *JETP Lett.* **82**, 447 (2005).
- <sup>11</sup>R. Kajimoto, H. Yoshizawa, H. Kawano, H. Kuwahara, Y. Tokura, K. Ohoyama, and M. Ohashi, *Phys. Rev. B* **60**, 9506 (1999).
- <sup>12</sup>J. van den Brink and D. Khomskii, *Phys. Rev. Lett.* **82**, 1016 (1999).
- <sup>13</sup>R. Mahendiran, M. R. Ibarra, A. Maignan, F. Millange, A. Arulraj, R. Mahesh, B. Raveau, and C. N. R. Rao, *Phys. Rev. Lett.* **82**, 2191 (1999).
- <sup>14</sup>D. Haskel, Y. C. Tseng, J. C. Lang, and S. Sinogeikin, *Rev. Sci. Instrum.* **78**, 083904 (2007).
- <sup>15</sup>D. D. Ragan, R. Gustavsen, and D. Schiferl, *J. Appl. Phys.* **72**, 5539 (1992).
- <sup>16</sup>D. L. Decker, *J. Appl. Phys.* **42**, 3239 (1971).
- <sup>17</sup><http://www.ill.eu/sites/fullprof/php/reference.html>.
- <sup>18</sup>H. Fujiwara, A. Sekiyama, A. Higashiya, K. Konoike, A. Tsunekawa, A. Yamasaki, A. Irizawa, S. Imada, T. Muro, K. Noda, H. Kuwahara, Y. Tokura, and S. Suga, *J. Electron Spectrosc. Relat. Phenom.* **144**, 807 (2005).
- <sup>19</sup>A. I. Abramovich, A. V. Michurin, O. Y. Gorbenko, and A. R. Kaul, *J. Phys.: Condens. Matter* **12**, L627 (2000).
- <sup>20</sup>C. Cui, T. A. Tyson, Z. Chen, and Z. Zhong, *Phys. Rev. B* **68**, 214417 (2003).
- <sup>21</sup>R. Makita, K. Tanaka, M. Kubotab and Y. Murakamic, *Acta Crystallogr. Sect. E* **64**, i77 (2008).
- <sup>22</sup>C. Sen, G. Alvarez, and E. Dagotto, *Phys. Rev. Lett.* **105**, 097203 (2010).
- <sup>23</sup>P. M. Woodward, T. Vogt, D. E. Cox, A. Arulraj, C. N. R. Rao, P. Karen, and A. K. Cheetham, *Chem. Mater.* **10**, 3652 (1998).
- <sup>24</sup>C. Meneghini, D. Levy, S. Mobilio, M. Ortolani, M. Nunez-Reguero, A. Kumar, and D. D. Sarma, *Phys. Rev. B* **65**, 012111 (2001).
- <sup>25</sup>M. Baldini, V. V. Struzhkin, A. F. Goncharov, P. Postorino, and W. L. Mao, *Phys. Rev. Lett.* **106**, 066402 (2011).